This is an open access article published under an ACS AuthorChoice License, which permits copying and redistribution of the article or any adaptations for non-commercial purposes.

THE JOURNAL OF PHYSICAL CHEMISTRY Letters

Letter

pubs.acs.org/JPCL

Induced Polarization Influences the Fundamental Forces in DNA Base Flipping

Justin A. Lemkul, Alexey Savelyev, and Alexander D. MacKerell, Jr.*

Department of Pharmaceutical Sciences, School of Pharmacy, University of Maryland, 20 Penn Street, Baltimore, Maryland 21201, United States

Supporting Information

ABSTRACT: Base flipping in DNA is an important process involved in genomic repair and epigenetic control of gene expression. The driving forces for these processes are not fully understood, especially in the context of the underlying dynamics of the DNA and solvent effects. We studied double-stranded DNA oligomers that have been previously characterized by imino proton exchange NMR using both additive and polarizable force fields. Our results highlight the importance of induced polarization on the base flipping process, yielding near-quantitative agreement with experimental measurements of the equilibrium between the base-paired and flipped states. Further, these simulations allow us to quantify for the first time the energetic implications of polarization on the flipping pathway. Free energy barriers to base flipping are reduced by changes in dipole moments of both the flipped bases that favor solvation of the bases in the open state and water molecules adjacent to the flipping base.

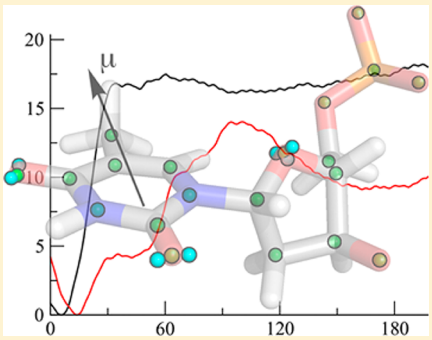

SECTION: Biophysical Chemistry and Biomolecules

The integrity and proper expression of an organism's genome are paramount to its survival. To this end, there exist numerous enzymes that modify DNA, either to repair mismatched or damaged nucleotides[1] or to exert epigenetic control of gene expression.[2] These enzymes distort the DNA double-helical structure to extrude the target nucleotide, allowing for various chemical modifications to be catalyzed. Local flexibility inherent to DNA is key to this process and allows the substrate base to be rotated up to 180° from its canonical Watson−Crick (WC) base-paired state. The driving forces for this process, in terms of both DNA flexibility and the effect of DNA-modifying enzymes, are not fully understood.

Through the flipping process, the target nucleotide experiences a range of microenvironments, from the relatively hydrophobic interior of the DNA double helix to interactions with the polyanionic backbone and aqueous solution. To accurately model this process via molecular dynamics (MD) simulations, the charge distribution of the flipped nucleotide must adjust to these different environments. Recently, a polarizable force field (FF) for DNA[3] based on the classical Drude oscillator model,[4−6] was presented. In the present work, we employ the Drude-2013 FF for DNA[3] in the study of base flipping to quantify the effects of induced polarization on this process. Two DNA sequences were studied, a palindromic decamer (5′-CTGGATCCAG-3′) and a dodecamer (5′-CTA-GGCGCCATG-3′), whose base flipping kinetics and equilibria have been characterized by imino proton exchange NMR.[7,8] Underlined bases in the preceding sequences indicate the position of the flipping bases. A previous study[9] calculated free energies and equilibrium constants for the same dodecameric sequence using the additive CHARMM27 (C27) FF,[10,11] serving as a useful reference for the additive FF used in the present work, CHARMM36 (C36).[10−13]

The approach in the present work is based on previous base-flipping studies.[9,14,15] A harmonic restraining potential was applied to a pseudodihedral angle (ϕ) defined by the flipped base, its sugar moiety, the sugar of the base to its 3′ side, and the 3′ base pair (Figure S1 in the Supporting Information). Umbrella sampling simulations were performed using this restraint in intervals of 5° along a 360° reaction coordinate from which potential of mean force (PMF) profiles were calculated using the weighted histogram analysis method (WHAM).[16] For complete details, see the Computational Methods.

PMF profiles for the flipping of all four bases under both C36 and Drude-2013 FFs are shown in Figure 1. Overall, the profiles are similar, with minima corresponding to the WC state in the vicinity of 0°, rapid increases in free energy as the bases flip out of either the minor or major grooves, and plateau regions from ∼60 to 300°. The relatively flat PMF profiles in the plateau region with C36 contrast with the more nuanced curves produced by the Drude-2013 FF, which indicate several local minima for T flipping and broad, shallow minima around the fully flipped states (ϕ = 180°) for T, A, and G flipping. The shapes of the PMF profiles for C flipping using C36 and the Drude-2013 FFs are similar, although the PMF curve for the

Received: May 13, 2014
Accepted: May 28, 2014
Published: May 28, 2014

 © 2014 American Chemical Society dx.doi.org/10.1021/jz5009517 | J. Phys. Chem. Lett. 2014, 5, 2077−2083

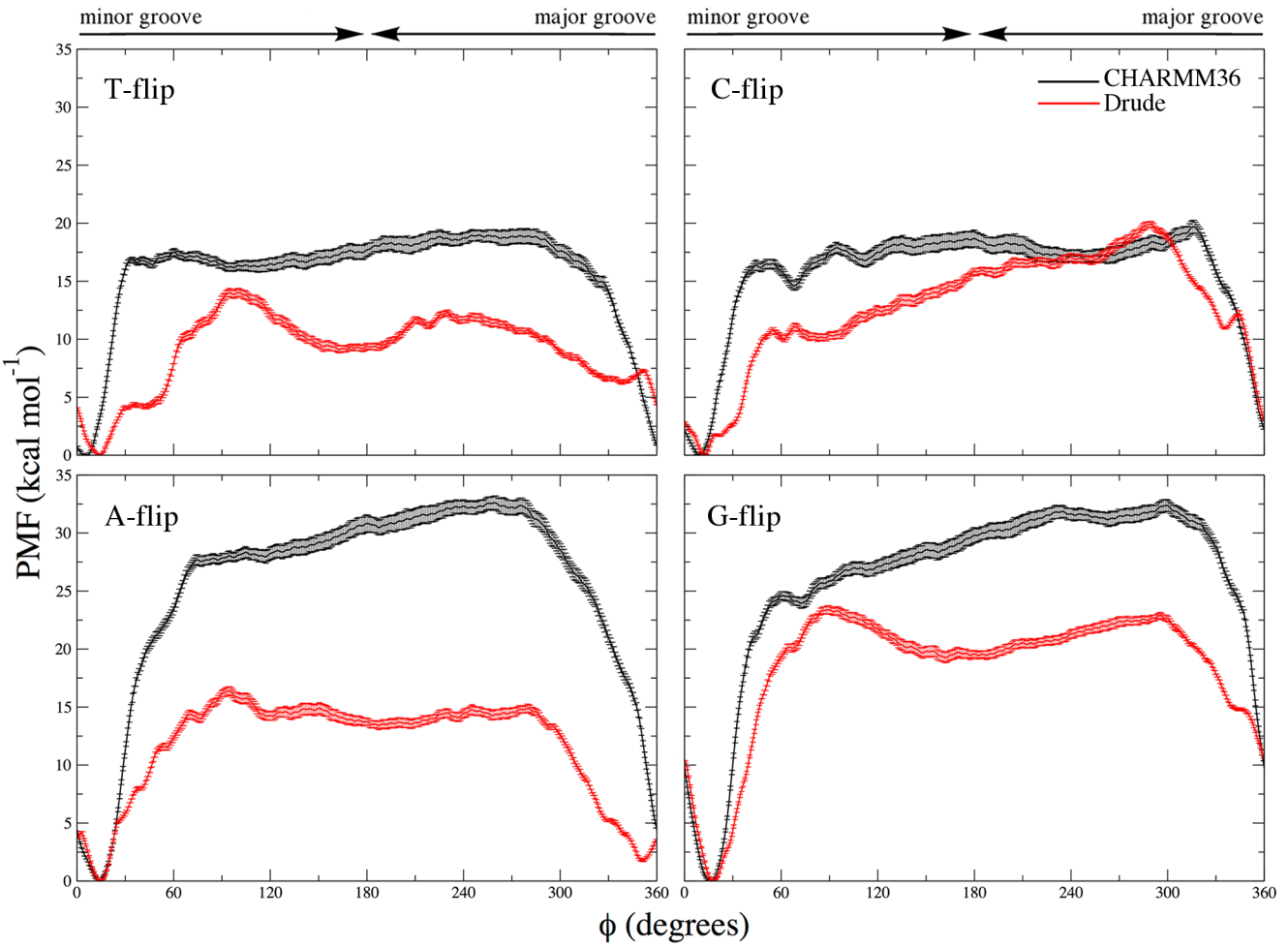

Figure 1. PMF profiles for all of the flipped bases using the C36 and Drude-2013 FFs. Error bars were produced using Monte Carlo bootstrap error analysis.[17]

Table 1. Calculated Values of K_{op} and Solvent-Accessible Ranges of the Reaction Coordinate

base pair	pseudodihedral open range		calculated K_{op}		experimental K_{op}
	C36	Drude	C36	Drude	
AT					
T flip	35−325°	35−350°	3.5×10^{-8}	4.0×10^{-6}	
A flip	40−345°	45−360°	2.0×10^{-15}	2.9×10^{-7}	
total AT			3.5×10^{-8}	4.3×10^{-6}	$(2.00 \pm 0.04) \times 10^{-5}$
GC					
C flip	40−335°	20−340°	1.3×10^{-8}	1.3×10^{-7}	
G flip	40−340°	40−355°	6.8×10^{-15}	1.4×10^{-12}	
total GC			1.3×10^{-8}	1.3×10^{-7}	$(4.8 \pm 0.7) \times 10^{-7}$

Drude-2013 FF is less symmetric than the one produced using C36 and shows a shallow local minimum around $\phi = 90°$.

In imino proton exchange NMR, the labeled proton exchanges with the solvent, implying that it is destabilized from its WC state. Solvent exposure occurs over a range of ϕ values during the base flipping process. Thus, the equilibrium constant for base opening in solution, K_{op}, can be calculated by integrating the Boltzmann-weighted, unbiased probabilities obtained from the PMF for the "open" (solvent-accessible) and "closed" (solvent-occluded) states (Table 1). The solvent-accessible surface area (SASA) of the imino group of thymine (N3) or guanine (N1) was calculated for each window, assigning an "open" state for any nonzero value of SASA.[9,14,15] Solvent exposure of these imino groups can result from flipping of the base itself or diffusion of water molecules into the void created by flipping of its WC partner. As such, the base-pair K_{op} is the sum of the two individual base K_{op} values.

The Drude-2013 FF produced base-pair K_{op} values in near quantitative agreement with the experimental data, while those produced by C36 were one to two orders of magnitude lower. The individual base K_{op} values for thymine and cytosine using C36 are consistent with previous results[9,14,15] using the C27 additive nucleic acid FF, which generally produced pyrimidine K_{op} values on the order of 10^{-11} to 10^{-7}. Unlike previous studies in which the purine K_{op} dominated the base-pair K_{op} value,[9,15] here the pyrimidines dominate base-pair K_{op} values

dx.doi.org/10.1021/jz5009517 | J. Phys. Chem. Lett. 2014, 5, 2077−2083

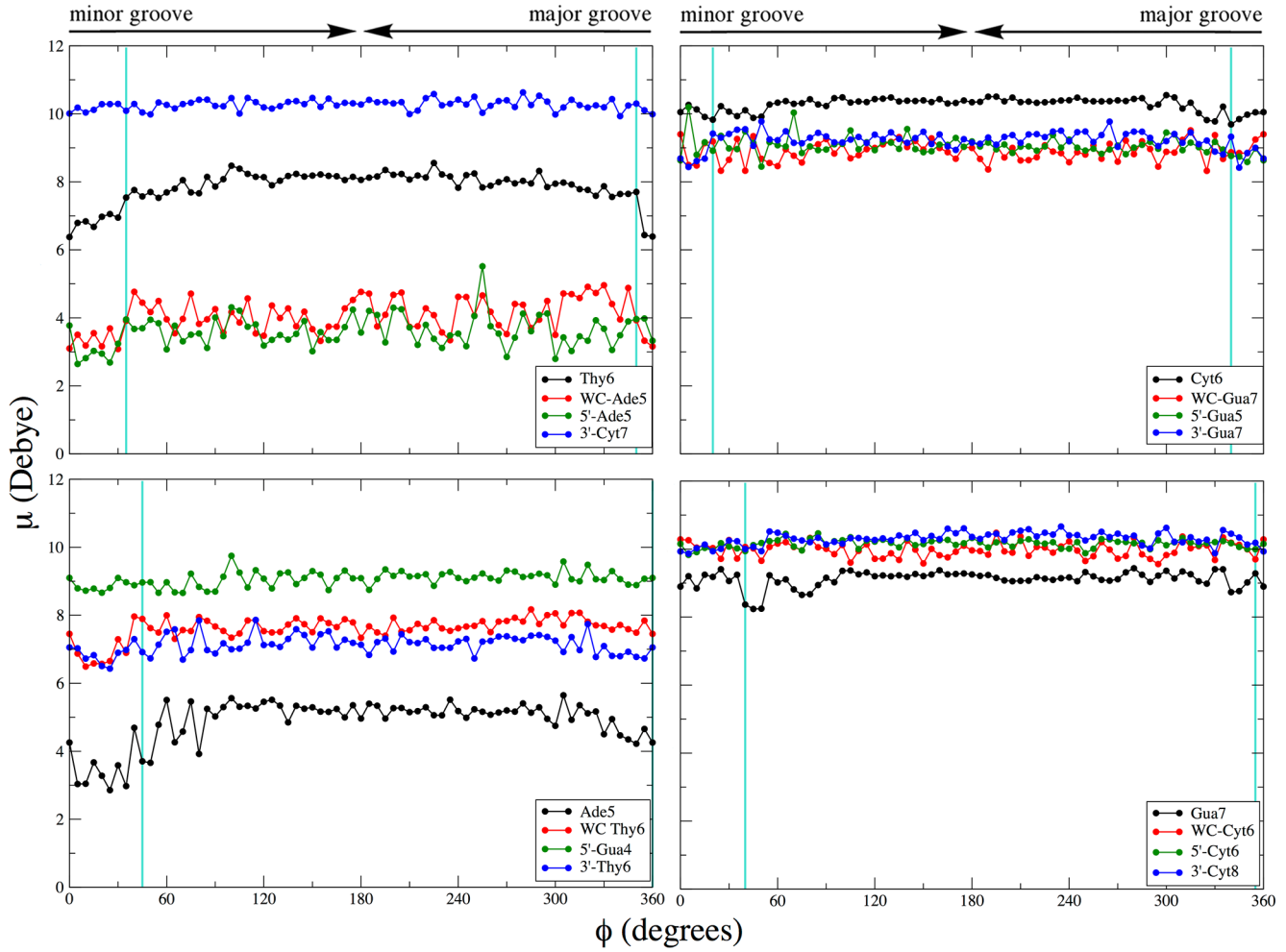

Figure 2. Dipole moments of the flipped bases, their WC partners, and bases to the 5′- and 3′-sides of the flipped bases. Vertical turquoise lines represent the boundaries of solvent accessibility, per Table 1. Standard deviations for each data point are approximately ±0.5 D.

under both FFs. Future studies will be required to determine if this is a sequence-specific phenomenon.

The smaller K_{op} values with C36 are associated with the higher barriers to flipping and overall higher energy of the plateau regions (Figure 1). The net result for C36 is base-pair K_{op} values that are approximately 35−500 times lower than those observed experimentally. The difference may be due to the reparametrization of several backbone and sugar dihedrals.[13] While the new parameters improved BI/BII equilibrium and sugar puckering properties in the context of duplex DNA relative to C27, the results obtained here indicate that the energies of flipped states are less favorable as a consequence of these new parameters. This outcome indicates that it is difficult to adequately parametrize additive FFs for DNA that accurately model both WC and flipped states, as has recently been noted.[18] In contrast, the polarizable Drude-2013 FF fares well in canonical DNA helices[3] as well as the extrahelical states studied here.

An obvious enhancement in the Drude-2013 FF that is effectively absent in additive FFs like C36 is dynamic electron redistribution in response to changes in local electric fields. Small variations in molecular dipole moments (μ) in additive FFs can arise due to simple changes in molecular geometry, but the magnitude of these changes is generally insignificant. To quantify the effect of induced polarization during base flipping, we calculated the dipole moments of the flipped base, the bases to either side of it, and the WC partner base in the opposite strand (Figure 2 and Figure S2 in the Supporting Information). Shown in Figure 2 are the respective base dipoles as a function of ϕ for the Drude polarizable FF, with the average changes in μ between open and closed states listed in Table 2. Plots of the additive C36 dipoles versus ϕ in Figure S2 in the Supporting Information show the values of μ of the selected bases to be systematically higher under the Drude-2013 FF than in C36, as previously reported.[3]

From Figure 2 and Table 2, it is evident that the base dipoles in the Drude-2013 FF simulations vary significantly in most

Table 2. Changes in Dipole Moments ($\Delta\mu$, in Debye) of Selected Bases Using the Drude-2013 FF[a]

base pair	flipped base	WC partner	5′-base	3′-base
AT				
T flip	0.96	0.43	0.33	0.12
A flip	1.45	0.66	0.18	0.37
GC				
C flip	0.30	−0.07	0.13	0.55
G flip	−0.02	−0.13	0.20	0.30

[a] $\Delta\mu$ is the difference between the time-averaged μ values over all open and closed states, $\Delta\mu = \langle\mu_{open}\rangle - \langle\mu_{closed}\rangle$, as demarcated by the boundaries of solvent accessibility in Figure 2.

dx.doi.org/10.1021/jz5009517 | J. Phys. Chem. Lett. 2014, 5, 2077−2083

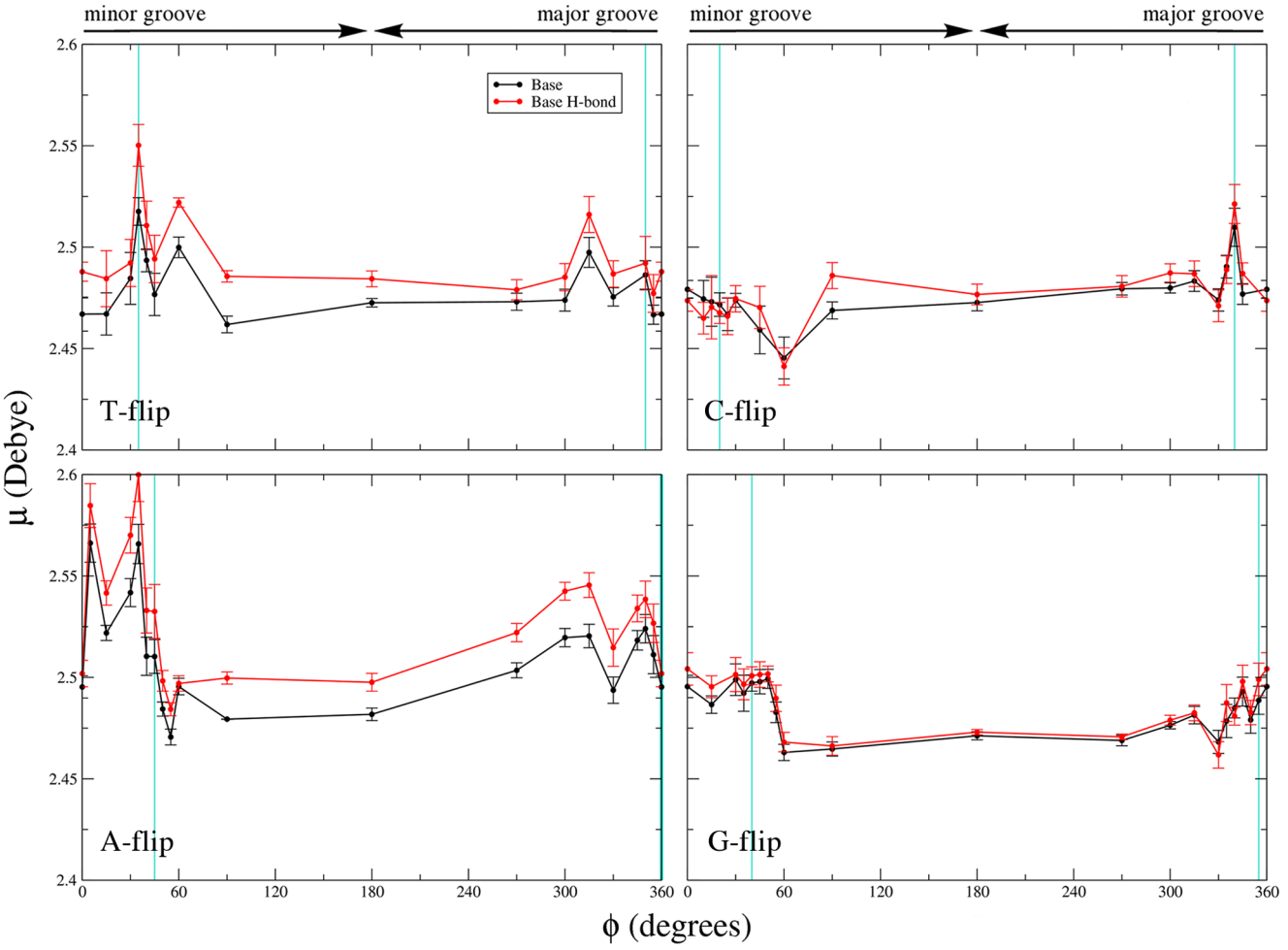

Figure 3. Values of μ_{wat} as a function of ϕ for water molecules in the first solvation shell around the flipping bases indicated in each panel. Vertical turquoise lines represent boundaries between WC and solvent-exposed states, as in Figure 2. Error bars are standard errors, calculated from five blocks of 100 ps over the final 500 ps of each simulation.

cases upon going from the WC to the flipped states, in contrast with the constant values observed with C36 (Figure S2 in the Supporting Information). Solvent exposure of either A or T dramatically increased the dipole of the flipped base, with some orientations more polarized in excess of 2 D relative to the WC base-paired state. C and G flipping resulted in smaller changes in the base dipoles than in the case of A and T flipping. The dipole moments of C and G are larger than those of A and T in WC base-paired states and do not respond as strongly to changes in environment as flipping occurs. For A and T flipping, the WC partner bases also experienced an increase in their dipoles, the magnitude of which was smaller than that of the flipped base itself. Changes in the dipole for bases to the 5′- and 3′-sides of the flipped bases were relatively small, with neighboring A and T bases more strongly affected than C or G. These effects may be sequence-dependent and merit additional scrutiny in future work.

Analysis of the dipole versus ϕ plots in Figure 2 in the transition regions, as indicated by the value of ϕ demarcating the boundaries of solvent accessibility, indicates some sharp variations. For example, there is a jump of ∼1.5 D in T as it flips through the major groove, while there is a decrease in the dipole of G as it moves beyond the solvent accessibility boundary through the minor groove, even though $\Delta\mu$ of G is small between the open and closed states (Table 2). Other examples include changes in the WC partner A and the 5′ stacked A in T flipping. These results indicate that alterations in the base dipoles in certain instances make important contributions to the energetics of barrier crossing.

In addition to the base dipole moments, we also examined the dipole moments of water molecules (μ_{wat}) in the first solvation shell around the flipping bases, with a particular focus on transitions between the WC and solvent-exposed states. The solvation shell was defined as any water molecule with an O atom within 3.5 Å of any base non-hydrogen atom. The solvation shell was further subdivided by considering waters interacting with hydrogen-bonding groups of the bases. Average values of μ_{wat} for waters in the first solvation shell as a function of ϕ are shown in Figure 3. The values of μ_{wat} largely followed the behavior of the base dipole moments (Figure 2). For A and T flipping, as the bases crossed the boundary between WC and solvent-exposed states, the base dipole moments increased, as did μ_{wat}. In general, hydrogen-bonded waters showed larger changes. For both A and T flipping, μ_{wat} for waters interacting with hydrogen-bonding groups increased by ∼0.06 D through the minor groove. Waters in the major groove were slightly less sensitive, with increases in μ_{wat} of ∼0.04 and ∼0.01 D for A and T flipping, respectively.

While C and G flipping led to small overall values of $\Delta\mu$ for the bases between the open and closed states (Table 2), base

dx.doi.org/10.1021/jz5009517 | J. Phys. Chem. Lett. 2014, 5, 2077−2083

Table 3. Time-Averaged Nonbonded Interaction Energy Differences (kcal mol^{-1}) between Flipped (ϕ = 180°) and WC States of the Flipping Unit (nucleoside and surrounding phosphodiester linkages and sugars; see text) and the Aqueous Solution (Unit−solution), the Remainder of the DNA (unit − DNA), and Both the Solution and Remaining DNA (total)[a]

	ΔE (unit−solution)		ΔE (unit − DNA)		ΔE (total)		$\Delta\Delta E$
	Drude	C36	Drude	C36	Drude	C36	(total)
T flip	−29.55	−14.74	26.66	23.82	−2.90	9.07	−11.97
A flip	−46.23	−32.20	30.55	33.51	−15.68	1.30	−16.98
C flip	−36.02	−21.69	41.29	30.92	5.27	9.23	−3.96
G flip	−49.37	−39.00	45.97	34.39	−3.40	−4.61	1.21

[a]$\Delta\Delta E$ is the difference between the total Drude and C36 total interaction energies differences.

dipole moments generally decreased slightly upon crossing the solvent accessibility barrier (Figure 2). Water molecules in the first solvation shell followed the same trend. While C flipping through the major groove led to an increase in μ_{wat}, flipping through the minor groove led to a decrease in μ_{wat}, in parallel with the base dipole moment. Similarly, G flipping led to decreases in μ_{wat} relative to the WC state, mirroring the decrease in base dipole moment observed upon entrance of G into the minor groove and the smaller decrease in base dipole moment through the major groove. The results of the μ_{wat} analysis indicate that solvating water molecules are sensitive to the orientation of the flipping bases, suggesting that changes in both base and water dipole moments contribute to the reduction in the free-energy barriers to flipping as compared with the additive FF.

Competing interactions between solvent and DNA contribute to the forces involved in base flipping, thereby impacting the equilibrium between the WC and flipped states. To better understand these interactions as well as how the changes in base dipoles in the Drude model lead to the better agreement with the NMR data for flipping, we determined changes in various energetic contributions along the flipping profile. For this analysis, we considered the interaction energies of a flipping unit (the full flipped nucleoside as well as the 5′- and 3′-sugars with their phosphodiester linkers) with both the solvent and the remainder of the DNA. (See the Supporting Information.) The differences in energy, ΔE, between the fully flipped (ϕ = 180°) and WC states are listed in Table 3. The values of $\Delta\Delta E$ for Drude-2013 versus C36 indicate that these contributions can be considerable, with the more favorable values with Drude-2013 qualitatively correlating with the lower free energies of the plateau region in the PMFs (Figure 1). For example, with T flipping, the solvation energy of the base becomes more favorable by −29.6 kcal/mol in the flipped state, with the polarizable model versus −14.7 kcal/mol for C36. Flipping of G is the only case for which the Drude-2013 FF predicts a less favorable $\Delta\Delta E$ during flipping than does C36. Interestingly, the values of $\Delta\mu$ for the flipping bases (Table 2) correlate linearly with the observed values of $\Delta\Delta E$ (R^2 = 0.994), suggesting that the response of the base dipole moment to the change in environment contributes to more favorable interactions with the environment in the polarizable FF, thereby favoring the flipped state. The exception to this trend is with G, which has the least favorable plateau free energies of the four systems studied. This outcome indicates that additional terms are contributing to the lowered free energies of the open states in the Drude model.

In conclusion, we have presented a first-of-its-kind application of a Drude polarizable FF to the study of DNA base flipping, elucidating several important aspects of the flipping pathways for A, C, T, and G that cannot be observed with traditional additive FFs. Explicit inclusion of polarization is particularly important in obtaining near-quantitative agreement with experimental base-opening K_{op} values. Variable dipole moments for the flipped bases contribute to a more favorable free-energy change along the flipping pathway due, in part, to more favorable interactions with the aqueous solution associated with increased base dipoles. Coupled to the variation of water dipole moments in the first solvation shell around the flipped bases, these effects dramatically reduce the free energy of the fully flipped states relative to the additive C36 FF. The outcomes of this study highlight the importance of including induced polarization in simulations of highly dynamic biomolecular processes that include significant structural changes such as DNA base flipping and may ultimately lead to a more detailed understanding of the mechanism by which enzymes facilitate this process.

COMPUTATIONAL METHODS

All simulations were carried out using CHARMM,[19] with the additive C36 or the polarizable Drude-2013 FFs. All simulated systems were initially prepared under the C36 additive FF. Each DNA double helix was solvated with TIP3P[20−22] water and neutralizing Na^+ ions in a periodic octahedral unit cell. Following energy minimization, each system was heated to 283.15 K, corresponding to the experimental conditions,[7,8] over 20 ps with weak harmonic restraints on all DNA heavy atoms. Restraints were removed, and temperature and pressure were held constant at 283.15 K using a Hoover thermostat[23] and 1.0 atm with the Langevin piston method,[24] respectively, for an additional 80 ps. All covalent bonds involving hydrogen atoms were constrained with SHAKE,[25] allowing an integration time step of 2 fs for C36 simulations and 1 fs for Drude-2013 simulations. Electrostatic interactions were calculated with the particle mesh Ewald method,[26,27] with the real-space contribution truncated at 12 Å. Lennard-Jones interactions were switched from 10 to 12 Å. Neighbor lists were updated within 14 Å.

Following equilibration, 72 configurations for umbrella sampling were generated using the miscellaneous mean field potential (MMFP) module of CHARMM. The reaction coordinate was a pseudodihedral angle (ϕ) described previously,[9,14,15] and an example is illustrated in Figure S1 in the Supporting Information. In brief, the four groups of atoms constituting the pseudodihedral angle are defined as the heavy atoms of the flipped base, its sugar ring, the sugar ring of the adjacent 3′-nucleotide, and the base pair to the 3′-side of the flipped base. Configurations were generated from 0 to 180° and from 0 to −180° in increments of 5° along the reaction coordinate, constituting flipping through both the minor and major grooves (Figure S1 in the Supporting Information), using

dx.doi.org/10.1021/jz5009517 | J. Phys. Chem. Lett. 2014, 5, 2077−2083

a force constant of 5000 kcal mol^{-1} rad^{-2}. At this point, for the polarizable simulations, lone pairs and Drude particles were added to the systems, a process that also converted TIP3P water into the polarizable SWM4-NDP model.[28] For Drude systems, an additional 50 ps of NPT equilibration was performed, and the selections defining the pseudodihedral angle also included the Drude particles associated with the non-hydrogen atoms.

Umbrella sampling calculations were performed on each of the 72 windows. The simulation time in each window was 1 ns for C36 simulations and 1.5 ns for Drude-2013 simulations, with all analysis performed over the final 500 ps. The biasing force constant during umbrella sampling was 250 kcal mol^{-1} rad^{-2}. PMF curves were generated using WHAM,[16] with a window dimension of 1° along the periodic reaction coordinate. Coordinates were saved every 1 ps for analysis; values of ϕ were output at each simulation step. Convergence was assessed by calculating the PMF profiles and associated K_{op} values over consecutive blocks of time during the simulations. Simulations were stopped when 500 ps of continuous time existed, such that PMF profiles had stabilized. PMF profiles over different blocks of time are shown in Figures S3 and S4 in the Supporting Information.

■ ASSOCIATED CONTENT

Ⓢ Supporting Information

Supporting methods. Definition of the pseudodihedral angle for thymine flipping. Dipole moments for selected bases as a function of the psuedodihedral, ϕ, for Drude and CHARMM36 systems. Convergence of PMF profiles for the C36 FF. Convergence of PMF profiles for the Drude-2013 FF. This material is available free of charge via the Internet at http://pubs.acs.org.

■ AUTHOR INFORMATION

Corresponding Author

*E-mail: alex@outerbanks.umaryland.edu. Phone: (410) 706-7442. Fax: (410) 706-5017.

Notes

The authors declare no competing financial interest.

■ ACKNOWLEDGMENTS

Financial support for this work was provided by NIH grants F32GM109632 (to J.A.L.) and GM051501 (to A.D.M.). Computing time on the XSEDE Blacklight supercomputer under allocation TG-MCA98N017 and computing resources from the University of Maryland Computer-Aided Drug Design Center are gratefully acknowledged. The authors thank Jing Huang for helpful discussions and assistance.

■ REFERENCES

(1) Wiebauer, K.; Jiricny, J. *In Vitro* Correction of G•T Mispairs to G•C Pairs in Nuclear Extracts from Human Cells. *Nature* **1989**, *339*, 234−236.

(2) Wu, S. C.; Zhang, Y. Active DNA Demethylation: Many Roads Lead to Rome. *Nat. Rev. Mol. Cell Biol.* **2010**, *11*, 607−620.

(3) Savelyev, A.; MacKerell, A. D., Jr. All-Atom Polarizable Force Field for DNA Based on the Classical Drude Oscillator Model. *J. Comput. Chem.* **2014**, *35*, 1219−1239.

(4) Drude, P.; Millikan, R. A.; Mann, R. C. *The Theory of Optics*; Longmans, Green, and Co.: New York, 1902.

(5) Waldman, M.; Gordon, R. G. Generalized Electron Gas-Drude Model Theory of Intermolecular Forces. *J. Chem. Phys.* **1979**, *71*, 1340−1352.

(6) Harder, E.; Anisimov, V. M.; Vorobyov, I. V.; Lopes, P. E. M.; Noskov, S. Y.; MacKerell, A. D., Jr.; Roux, B. Atomic Level Anisotropy in the Electrostatic Modeling of Lone Pairs for a Polarizable Force Field Based on the Classical Drude Oscillator. *J. Chem. Theory. Comput.* **2006**, *2*, 1587−1597.

(7) Cao, C.; Jiang, Y. L.; Krosky, D. J.; Stivers, J. T. The Catalytic Power of Uracil DNA Glycosylase in the Opening of Thymine Base Pairs. *J. Am. Chem. Soc.* **2006**, *128*, 13034−13035.

(8) Dornberger, U.; Leijon, M.; Fritzsche, H. High Base Pair Opening Rates in Tracts of Gc Base Pairs. *J. Biol. Chem.* **1999**, *274*, 6957−6962.

(9) Priyakumar, U. D.; MacKerell, A. D., Jr. NMR Imino Proton Exchange Experiments on Duplex DNA Primarily Monitor the Opening of Purine Bases. *J. Am. Chem. Soc.* **2006**, *128*, 678−679.

(10) Foloppe, N.; MacKerell, A. D., Jr. All-Atom Empirical Force Field for Nucleic Acids: I. Parameter Optimization Based on Small Molecular and Condensed Phase Macromolecular Target Data. *J. Comput. Chem.* **2000**, *21*, 86−104.

(11) MacKerell, A. D., Jr.; Banavali, N. K. All-Atom Empirical Force Field for Nucleic Acids: Ii. Application to Molecular Dynamics Simulations of DNA and RNA in Solution. *J. Comput. Chem.* **2000**, *21*, 105−120.

(12) Denning, E. J.; Priyakumar, U. D.; Nilsson, L.; MacKerell, A. D., Jr. Impact of 2′-Hydroxyl Sampling on the Conformational Properties of RNA: Update of the CHARMM All-Atom Additive Force Field for RNA. *J. Comput. Chem.* **2011**, *32*, 1929−1943.

(13) Hart, K.; Foloppe, N.; Baker, C. M.; Denning, E. J.; Nilsson, L.; MacKerell, A. D., Jr. Optimization of the CHARMM Additive Force Field for DNA: Improved Treatment of the BI/BII Conformational Ensemble. *J. Chem. Theory. Comput.* **2011**, *8*, 348−362.

(14) Banavali, N. K.; MacKerell, A. D., Jr. Free Energy and Structural Pathways of Base Flipping in a DNA GCGC Containing Sequence. *J. Mol. Biol.* **2002**, *319*, 141−160.

(15) Priyakumar, U. D.; MacKerell, A. D., Jr. Base Flipping in a GCGC Containing DNA Dodecamer: A Comparative Study of the Performance of the Nucleic Acid Force Fields, CHARMM, AMBER, and BMS. *J. Chem. Theory. Comput.* **2006**, *2*, 187−200.

(16) Kumar, S.; Bouzida, D.; Swendsen, R. H.; Kollman, P. A.; Rosenberg, J. M. The Weighted Histogram Analysis Method for Free-Energy Calculations in Biomolecules. I. The Method. *J. Comput. Chem.* **1992**, *13*, 1011−1021.

(17) Efron, B.; Tibshirani, R. J. *An Introduction to the Bootstrap*; Chapman & Hall/CRC: New York, 1993.

(18) Šponer, J.; Banás, P.; Jurečka, P.; Zgarbová, M.; Kührová, P.; Havrila, M.; Krepl, M.; Stadlbauer, P.; Otyepka, M. Molecular Dynamics Simulations of Nucleic Acids. From Tetranucleotides to the Ribosome. *J. Phys. Chem. Lett.* **2014**, *5*, 1771−1782.

(19) Brooks, B. R.; Brooks, C. L., III; MacKerell, A. D., Jr.; Nilsson, L.; Petrella, R. J.; Roux, B.; Wom, Y.; Archontis, G.; Bartels, C.; Boresch, S.; et al. CHARMM: The Biomolecular Simulation Program. *J. Comput. Chem.* **2009**, *30*, 1545−1614.

(20) Jorgensen, W. L.; Chandrasekhar, J.; Madura, J. D.; Impey, R. W.; Klein, M. L. Comparison of Simple Potential Functions for Simulating Liquid Water. *J. Chem. Phys.* **1983**, *79*, 926−935.

(21) Durell, S. R.; Brooks, B. R.; Ben-Naim, A. Solvent-Induced Forces between Two Hydrophilic Groups. *J. Phys. Chem.* **1994**, *98*, 2198−2202.

(22) Neria, E.; Fischer, S.; Karplus, M. Simulation of Activation Free Energies in Molecular Systems. *J. Chem. Phys.* **1996**, *105*, 1902.

(23) Hoover, W. G. Canonical Dynamics: Equilibrium Phase-Space Distributions. *Phys. Rev. A: At. Mol. Opt. Phys.* **1985**, *31*, 1695−1697.

(24) Feller, S. E.; Zhang, Y.; Pastor, R. W.; Brooks, B. R. Constant Pressure Molecular Dynamics Simulation: The Langevin Piston Method. *J. Chem. Phys.* **1995**, *103*, 4613.

(25) Ryckaert, J.-P.; Ciccotti, G.; Berendsen, H. J. C. Numerical Integration of the Cartesian Equations of Motion of a System with

Constraints: Molecular Dynamics of *N*-Alkanes. *J. Comput. Phys.* **1977**, *23*, 327−341.
(26) Darden, T.; York, D.; Pedersen, L. Particle Mesh Ewald: An N·Log(N) Method for Ewald Sums in Large Systems. *J. Chem. Phys.* **1993**, *98*, 10089−10092.
(27) Essmann, U.; Perera, L.; Berkowitz, M. L.; Darden, T.; Lee, H.; Pedersen, L. G. A Smooth Particle Mesh Ewald Method. *J. Chem. Phys.* **1995**, *103*, 8577−8593.
(28) Lamoureux, G.; Harder, E.; Vorobyov, I. V.; Roux, B.; MacKerell, A. D., Jr. A Polarizable Model of Water for Molecular Dynamics Simulations of Biomolecules. *Chem. Phys. Lett.* **2006**, *418*, 245−249.